

Some Invariant Solutions of the Savage–Hutter Model for Granular Avalanches

V. CHUGUNOV[†], J.M.N.T. GRAY[‡] and K. HUTTER^{*}

[†] Kazan State University, Kazan 420008, Russia

E-mail: chug@ksu.ru

[‡] Department of Mathematics, University of Manchester, Manchester M13 9PL U.K.

E-mail: ngray@man.ac.uk

^{*} Institut für Mechanik, Technische Universität Darmstadt, Darmstadt 64289, Germany

E-mail: hutter@mechanik.tu-darmstadt.de

Consider the spatially one-dimensional time dependent system of equations, obtained by Savage and Hutter, which describes the gravity-driven free surface flow of granular avalanches. All the similarity solutions of this system are found by means of the group analysis. The results of computing experiments are reduced and their physical treatment is considered.

1 Introduction

The most general non-dimensional form of the Savage–Hutter theory, which includes both the [1] and [2] formulations, can be obtained by reducing the theory of Gray *et al.* [3] to one-dimension. The time-dependent depth integrated mass and downslope momentum balance equations are

$$\frac{\partial h}{\partial t} + \frac{\partial Q}{\partial x} = 0, \tag{1}$$

$$\frac{\partial Q}{\partial t} + \frac{\partial}{\partial x} (Q^2 h^{-1}) + \frac{\partial}{\partial x} (\beta h^2 / 2) = h s, \tag{2}$$

where h is the avalanche thickness, Q is the depth averaged downslope volume flux and x is the curvilinear downslope coordinate. The source term s on the right-hand side of (2) is composed of the downslope component of gravitational acceleration, the Coulomb sliding friction with basal angle of friction δ and gradients of the basal topography height, b , above the curvilinear coordinate system. It takes the form

$$s = \sin \zeta - Q|Q|^{-1} \tan \delta (\cos \zeta + \lambda \kappa Q^2 h^{-2}) - \varepsilon \cos \zeta \frac{\partial b}{\partial x}, \tag{3}$$

where ζ is inclination angle of the curvilinear coordinate to the horizontal and $\kappa = -\partial\zeta/\partial x$ is the curvature. In a typical avalanche the thickness magnitude H^* is much smaller than its length L^* , which is reflected in the small non-dimensional parameter $\varepsilon = H^*/L^*$. The shallowness assumption also requires that typical avalanche lengths are shorter than the radius of curvature R^* of the curvilinear coordinate, which introduces the second non-dimensional parameter $\lambda = L^*/R^*$. The function

$$\beta = \varepsilon K \cos \zeta, \tag{4}$$

where the earth pressure coefficient K was proposed to take two limiting states K_{act} and K_{pas} associated with extensive ($\partial u/\partial x \geq 0$) and compressive ($\partial u/\partial x < 0$) motions, respectively. Savage & Hutter [1] showed that

$$K_{\text{act/pas}} = 2 \sec^2 \phi \left(1 \mp \{1 - \cos^2 \phi \sec^2 \delta\}^{1/2} \right) - 1, \tag{5}$$

where ϕ is the internal angle of friction of the granular material.

Recent experiments suggest that the jump in K at $\partial u/\partial x = 0$ is unrealistic and that a slowly varying function or a constant earth pressure coefficient is more realistic. In this paper it is therefore assumed that K is constant. It shall also be assumed that the slope is flat, $b \equiv 0$, and inclined at a constant angle ζ to the horizontal. This implies that the curvature $\kappa = 0$ and that β is constant. In addition placing the restriction that the volume flux $Q > 0$ implies that the source term $s = s_0$ is also constant.

Three exact solutions to the system of equations (1)–(2) are currently known. These are the parabolic cap similarity solution and the ‘M’-wave solutions, derived by Savage & Hutter [1], and the travelling shock wave solution [4] on a non-accelerative slope. In this paper we seek to find further simple solutions of physical interest.

2 Results of the group analysis and construction of the invariant solutions

Consider a moving coordinate system

$$\eta = x - s_0 t^2/2. \quad (6)$$

The relative flux \widehat{Q} in the moving coordinate system is then given by

$$\widehat{Q} = Q - h s_0 t. \quad (7)$$

In the new variable the system (1), (2) may be written in the form

$$\frac{\partial h}{\partial t} + \frac{\partial \widehat{Q}}{\partial \eta} = 0, \quad (8)$$

$$\frac{\partial \widehat{Q}}{\partial t} + \frac{\partial (\widehat{Q}^2 h^{-1})}{\partial \eta} = -\frac{\partial (0.5\beta h^2)}{\partial \eta}. \quad (9)$$

If to introduce the relative rate \widehat{u} by the relation $\widehat{u} = \widehat{Q}/h$ then the system (8), (9) takes the form

$$\frac{\partial h}{\partial t} + \frac{\partial \widehat{u} h}{\partial \eta} = 0, \quad (10)$$

$$\frac{\partial \widehat{u}}{\partial t} + \widehat{u} \frac{\partial \widehat{u}}{\partial \eta} + \beta \frac{\partial h}{\partial \eta} = 0. \quad (11)$$

These equations coincide with the shallow-water equations considered by Ibragimov [5]. The system (10), (11) admits the symmetry Lie algebra $L_5 \oplus L_\infty$ [6]. Used this algebra and the relation $\widehat{u} = \widehat{Q}/h$ we find the following basis of Lie algebra for (8), (9)

$$\begin{aligned} X_1 &= \frac{\partial}{\partial t}, & X_2 &= \frac{\partial}{\partial \eta}, & X_3 &= t \frac{\partial}{\partial t} + \eta \frac{\partial}{\partial \eta}, & X_4 &= \eta \frac{\partial}{\partial \eta} + 2h \frac{\partial}{\partial h} + 3\widehat{Q} \frac{\partial}{\partial \widehat{Q}}, \\ X_5 &= t \frac{\partial}{\partial \eta} + h \frac{\partial}{\partial \widehat{Q}}, & X_\infty &= Z(\widehat{u}, h) \frac{\partial}{\partial \eta} + T(\widehat{u}, h) \frac{\partial}{\partial t}, \end{aligned}$$

where the functions $Z(\widehat{u}, h)$, $T(\widehat{u}, h)$ are defined by the linear equations

$$Z_{\widehat{u}} - \widehat{u} T_{\widehat{u}} + h T_h = 0, \quad Z_h - \widehat{u} T_h + \beta T_{\widehat{u}} = 0.$$

Here $\hat{u} = \hat{Q}/h$. In this paper we will consider only the invariant solutions with respect to the stretching transformations of η and t . Evidently, the stretching transformations of η and t are generated by the infinitesimal operator (or generator) $X \in L_5$

$$X = (\mu - 1)X_3 + X_4. \quad (12)$$

Any invariant function f solves the partial differential equation $Xf = 0$ [7]. Therefore the basis of invariants is furnished by

$$\begin{aligned} J_1 &= \eta t^{-\mu/(\mu-1)}, & J_2 &= ht^{-2/(\mu-1)}, & J_3 &= \hat{Q}t^{-3/(\mu-1)}, & \mu &\neq 1, \\ J_1 &= t, & J_2 &= h\eta^{-2}, & J_3 &= \hat{Q}\eta^{-3}, & \mu &= 1. \end{aligned}$$

Consequently, the invariant solution of the system (8), (9) with respect to the group, generated by (12), are defined in the form

$$h = \eta^2 F(t), \quad \hat{Q} = \eta^3 \Phi(t), \quad \mu = 1, \quad (13)$$

where the functions $F(t)$ and $\Phi(t)$ are found by the equations

$$\dot{\Phi} + 4\Phi^2 F^{-1} + 2\beta F^2 = 0, \quad \dot{F} + 3\Phi = 0, \quad (14)$$

where the dot denotes differentiation with respect to t , and

$$h = t^{2/(\mu-1)} f(z), \quad \hat{Q} = t^{3/(\mu-1)} q(z), \quad \mu \neq 1, \quad (15)$$

where $z = J_1 = \eta t^{-\mu/(\mu-1)}$, and the functions $f(z)$, $q(z)$ satisfy the following system

$$\frac{3}{\mu-1}q - \frac{\mu}{\mu-1}q'z + (q^2 f^{-1} + 0.5\beta f^2)' = 0, \quad (16)$$

$$\frac{2}{\mu-1}f - \frac{\mu}{\mu-1}zf' + q' = 0. \quad (17)$$

Here, the stroke denotes differentiation with respect to z . Note that the system (16), (17), and (14) represent ordinary differential equations, and the relative velocity $\hat{u} = \eta\Phi(t)/F(t)$ for $\mu = 1$ and $\hat{u} = t^{1/(\mu-1)}q(z)/f(z)$ for $\mu \neq 1$.

3 Qualitative analysis of the family of the self-similar solution

3.1 The case $\mu = 1$

The system (14) may be solved exactly. It easy to obtain

$$\pm t = \begin{cases} \frac{3a}{2b^{3/2}} \ln \left[\left(\frac{\theta+1}{\theta_0+1} \right) \left(\frac{\theta_0-1}{\theta-1} \right) \right] - \frac{3}{\sqrt{b}} \left(\frac{\theta}{F^{1/3}} - \frac{\theta_0}{F_0^{1/3}} \right), & b > 0, \\ \frac{2}{\sqrt{a}} \left(F_0^{-1/2} - F^{-1/2} \right), & b = 0, \\ \frac{3a}{(-b)^{3/2}} \left(\tan^{-1} \psi - \tan^{-1} \psi_0 \right) + \frac{3}{\sqrt{-b}} \left(\frac{\psi}{F^{1/3}} - \frac{\psi_0}{F_0^{1/3}} \right), & b < 0, \end{cases} \quad (18)$$

where $a = 36\beta > 0$, $\theta = ((aF^{1/3} + b)/b)^{1/2}$ and $\psi = ((aF^{1/3} + b)/(-b))^{1/2}$, and θ_0 and ψ_0 are the same functions evaluated at $F = F_0$; b , F_0 are the constants of integration. For $\mu = 1$ the exact solution of equations (1) and (2) is of the form

$$h = (x - s_0 t^2/2)^2 F(t), \quad Q = h s_0 t + (x - s_0 t^2/2)^3 \Phi(t). \quad (19)$$

where $\Phi(t) = -\dot{F}(t)/3$, and F is defined by (18). Evidently, the function $F(t)$ has a growing and decaying branch corresponding to the positive and negative roots in (18). The growing branches are particularly interesting as they imply that the avalanche thickness can increase without bound within a finite period of time for all choices of the parameter b . In the case $b < 0$ the solution degenerates for $F < F^* = (-b/a)^3$.

3.2 The case $\mu = -2$

Equation (17) can be integrated directly when $\mu = -2$ to give

$$q = 2fz/3 + c_1, \quad (20)$$

where c_1 is an arbitrary constant. Substituting the volume flux from (20) the momentum balance (16) reduces to

$$f' = f^2(c_1/3 - 2zf/9)(c_1^2 - \beta f^3)^{-1}. \quad (21)$$

In the case $c_1 = 0$ equation (21) can be integrated to give

$$f(z) = (9\beta)^{-1}z^2 + c_2, \quad (22)$$

where c_2 is an arbitrary constant. The exact solution of (1), (2) in this case is

$$h = t^{-2/3} \left[(9\beta)^{-1} (x - s_0 t^2/2)^2 t^{-4/3} + c_2 \right], \quad (23)$$

$$Q = h s_0 t + 2t^{-1} \left[(9\beta)^{-1} (x - s_0 t^2/2)^3 t^{-2} + c_2 (x - s_0 t^2/2) t^{-2/3} \right] / 3. \quad (24)$$

Let us now consider more general solutions for the case $\mu = -2$ when $c_1 \neq 0$ in equation (21). It is convenient to introduce new variables y , p and ζ for f , q and z by the scalings

$$f = c_1 y (c_1 \beta)^{-1/3}, \quad q = c_1 p, \quad z = 3(c_1 \beta)^{1/3} \zeta, \quad (25)$$

which transform (21) into a parameter independent form

$$\frac{\partial y}{\partial \zeta} = y^2 (1 - 2\zeta y) (1 - y^3)^{-1}. \quad (26)$$

The avalanche thickness is non-negative and we therefore restrict attention to the domain $y \geq 0$, $-\infty < \zeta < \infty$. The solutions of equation (26) are illustrated in Fig. 1. On the line $y = 1$, the gradient $\partial y / \partial \zeta \rightarrow \pm\infty$ for all points except one, where $1 - 2\zeta y = 0$. Consequently, the point $\zeta = 1/2$, $y = 1$ is a singular point. The asymptotic behaviour of the solution in the vicinity of the line $y = 1$ is described by formula, which can be obtain from (26),

$$y = 1 \pm \sqrt{2[(\zeta - \zeta_0)(\zeta + \zeta_0 - 1)]/3}, \quad \zeta \rightarrow \zeta_0, \quad y \rightarrow 1. \quad (27)$$

If $\zeta_0 = 1/2$ then

$$y = 1 \pm \sqrt{2/3}(\zeta - 1/2), \quad \zeta \rightarrow 1/2, \quad y \rightarrow 1. \quad (28)$$

The singular point $(1/2, 1)$ is a saddle point. On the line $y = 1/(2\zeta)$ the gradient $\partial y / \partial \zeta = 0$. Therefore, in the points of this line the function $y(\zeta)$ assumes an extremum. In the region $y < 1$ $y(\zeta)$ has maximum and when $y > 1$, $y(\zeta)$ has a minimum. When $\zeta \rightarrow \pm\infty$, two asymptotic formulas emerge, first

$$\zeta \rightarrow \infty, \quad y \rightarrow 1/\zeta; \quad \zeta \rightarrow -\infty, \quad y \rightarrow -1/(2\zeta) \quad (29)$$

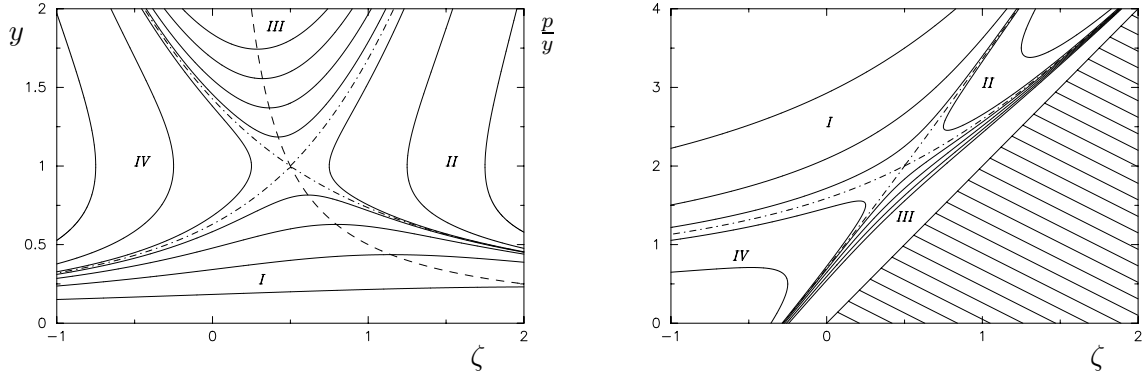


Figure 1. Four classes of asymmetric thickness, y , and velocity, p/y , solutions are illustrated as a function of ζ and labelled I – IV . The separatrix between the solution domains is indicated with the dot-dash curve and the dashed line indicates where the first derivative of the thickness $\partial y/\partial \zeta = 0$. There are no solutions in the hashed region.

for the region $y > 1$, and second

$$\zeta \rightarrow \pm\infty, \quad y \rightarrow \zeta^2, \quad (30)$$

for the region $y < 1$.

The curves, which pass through the singular point $(1/2, 1)$, divide the domain into the four parts. Each part has its own family of solutions of (26), which are denoted by I , II , III , IV (see Fig. 1). The families I – IV together with relations (6), (7), (15), (20), (25) define the various solutions of the system (1), (2). From a physical point of view family I is interesting for the motion of avalanches. Using this family we can construct the solution for various concrete situations.

Let us write the considered invariant solution for $\mu = -2$ and $c_1 \neq 0$ in the form

$$h(x, t) = (t + t_0)^{-2/3} \frac{c_1}{(c_1 \beta)^{1/3}} y \left[\frac{x - 0.5s_0(t + t_0)^2}{3(c_1 \beta)^{1/3}(t + t_0)^{2/3}} \right], \quad (31)$$

$$Q(x, t) = hs_0(t + t_0) + (t + t_0)^{-1} [c_1 + 2(x - 0.5s_0(t + t_0)^2)h(x, t)/3], \quad (32)$$

where $y(\zeta) \in I, II, III, IV$ and t_0, c_1 are arbitrary constants.

4 Results of the calculations, physical interpretation

4.1 Example 1. M-waves

The solutions (23), (24) was found using a separable variable approach by Savage & Hutter [1], who called it an “M”-wave. The name arose from the shape of a truncated solution

$$h(z, t) = \begin{cases} t^{-2/3} f(z), & |z| \leq 1, \\ 0, & |z| > 1, \end{cases} \quad (33)$$

which connected a finite part of the solution (22) with regions of zero thickness and flux on either side. At $z = \pm 1$ there are jump discontinuities in both the thickness and the flux, which should satisfy the mass and momentum jump conditions. They are obtained from the system (1), (2)

$$x'_j[h] - [Q] = 0, \quad x'_j[Q] - [Q^2 h^{-1} + \beta h^2/2] = 0, \quad (34)$$

where x_j is the position and x'_j is the normal velocity of the discontinuity, the jump bracket $[[f]] = f^+ - f^-$ and $f^\pm = f(x_j \pm 0)$. As we shall now show this is not the case. Assuming that on the positive side of the discontinuity $h^+ \neq 0$ and $Q^+ \neq 0$ and that on the negative side $h^- = Q^- = 0$ the jump conditions 34 imply

$$x'_j h^+ - Q^+ = 0, \quad x'_j Q^+ - (Q^+)^2/h^+ - \beta(h^+)^2/2 = 0. \quad (35)$$

Mass balance therefore requires that $x'_j = Q^+/h^+$ and if this is substituted in the momentum jump condition we find that $h^+ = 0$ contradicting our original assumption that $h^+ \neq 0$. The jump conditions are therefore not satisfied by the truncated M-wave solution (33), and expansion fans develop at the jumps.

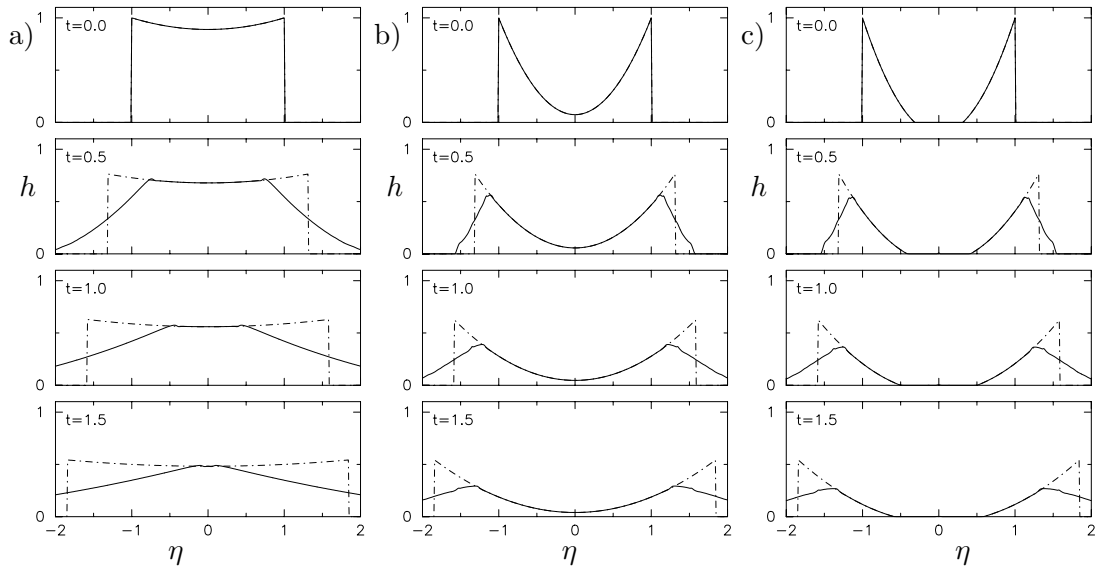


Figure 2. The temporal and spatial evolution of the avalanche thickness for the cases (a) $\beta = 1.0$, (b) $\beta = 0.12$ and (c) $\beta = 0.1$ are illustrated. The constant $c_2 = 1 - (9\beta)^{-1}$ to ensure that $h(\pm 1) = 1$. The solid line shows the computed solution in the accelerating coordinate system η and the dot-dash line shows the exact solution. Time is measured relative to initial conditions and the M-wave is evaluated at a finite time $t_0 = 1$.

To understand the collapse of the truncated M-wave in greater detail a series of numerical simulations have been performed using a Total Variational Diminishing Lax Friedrich's scheme [4]. This is a shock capturing method that has been extensively tested against the parabolic cap solution and the travelling shock solution. Fig. 2 shows the M-wave (33) and the numerical solutions for the avalanche thickness for various β at a sequence of time-steps in the accelerated coordinate system, η . The constant $c_2 = 1 - (9\beta)^{-1}$ to ensure that $h(\pm 1) = 1$. In each case the M-wave spreads out laterally, diminishing in height, and close to the discontinuities the shock expands as expected. The overlap domain, where the M-wave (33) and the computed solution are in close agreement, can either expand or contract in the physical domain. For $\beta = 1$ the overlap region decreases with time and the M-wave is destroyed in finite time. However, for thin avalanches where the aspect ratio $\varepsilon \ll 1$, and hence $\beta \ll 1$, the overlap domain expands in the physical domain despite the collapse close to the discontinuities. This is because the stretching of the solution is faster than the inward propagation speed of the disturbance from the discontinuities.

For $c_2 < 0$ the M-wave solution (33) contains regions of negative thickness. In this case the M-wave can be linked to the trivial solution $h \equiv 0$ using the jump conditions (34). This time, however, because the thicknesses and fluxes are zero on both sides of the discontinuity, the jump

conditions are trivially satisfied. Case (c) in Fig. 2 shows the evolution of such an M-wave for the case $\beta = 0.1$.

These numerical simulations demonstrate that for shallow avalanches, in which $\beta \ll 1$, the invariant stretching solutions may exist over an expanding region in the physical domain even though they may not satisfy boundary conditions at the ends.

4.2 Example 2. Evolution of the wave

Let us consider a second example: it assumes that the initial instant the avalanche thickness distribution is described by the formula

$$h_0 = \frac{s_0}{2\beta x_0} \left(\frac{H_0}{3} \right)^2 y \left(\frac{x - x_0}{H_0} \right), \quad (36)$$

where H_0, x_0 are known parameters and the function $y(\zeta)$ is one of the family I (Fig. 3). This profile has a maximum at $x = x_{\max}$. For example, $y(\zeta)$ is a function which has the maximum in the point $\zeta_{\max} = 1$ ($y_{\max} = 0.5$). Therefore, $x_{\max} = x_0 + H_0$ and $h_{0\max} = s_0 H_0^2 / (16\beta x_0)$. $h_{0\max}$ is the initial amplitude of the wave. The mathematical model for this problem is the Cauchy problem for the system (1), (2) with the initial condition (36).

The solution of this problem is described by the formulas (31), (32) with the constants c_1, t_0 and function $y(\zeta)$ which are defined by comparison of expression (31) with (36) at $t = 0$. Fig. 3 a) shows the evolution of the wave with time; the calculations were performed with the following values of the parameters: $\zeta = 45^\circ, \delta = 30^\circ, s_0 = 0.2989, \beta = 0.1, x_0 = 0.1, H_0 = 1$. Fig. 3 b) displays the corresponding behaviour of the mass flux.

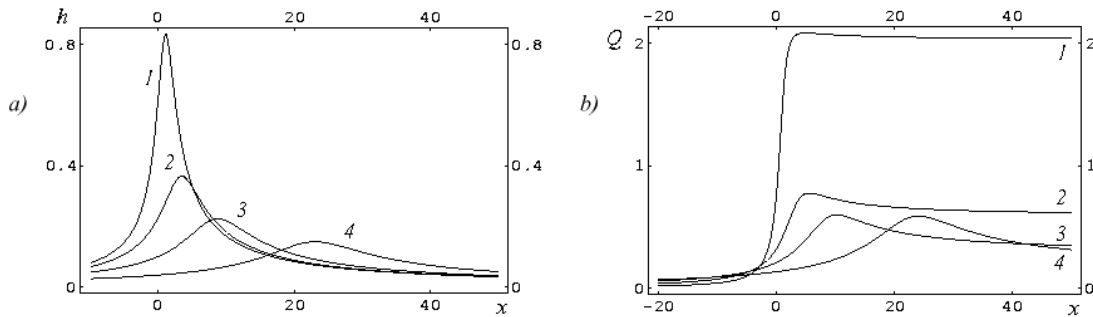


Figure 3. Evolution of the wave a) and the mass flux b) for (31), (32) (1 – $t = 0$, 2 – $t = 2$, 3 – $t = 5$, 4 – $t = 10$).

4.3 Example 3. Evolution of the wave during the “time of the life”

Let us consider the situation when the initial wave begins to grow and moves contrary to the downslope direction. It is possible when the initial profile of the thickness is described by the expression

$$h_0 = AY \left(\frac{x - x_0}{\lambda_0} \right), \quad Y(\zeta) = \frac{1}{y_{\max}} y(\zeta), \quad y \in I, \quad (37)$$

where A is an amplitude, λ_0 is a length of the wave, x_0 is a parameter, and the mass flux is $Q_\infty = -q_\infty(t_0 - t)^{-1} < 0$ in the right side of the wave when $x \rightarrow \infty$, and $Q_{-\infty} = 0$ when

$x \rightarrow -\infty$. In order to construct the solution for this situation we again take the invariant solution (31), (32). It is easy to check that the system (1), (2) admits the transformations

$$Q = -\bar{Q}, \quad h = \bar{h}, \quad t = -\bar{t}, \quad x = \bar{x}; \quad (38)$$

$$Q = \bar{Q}, \quad h = \bar{h}, \quad t = \bar{t} + t_0, \quad x = \bar{x}. \quad (39)$$

Consequently, the any solution of the equations (1), (2) which was transformed by the (38), (39) again is a solution of the system (1), (2). Therefore from (31), (32) we have

$$h(x, t) = (t_0 - t)^{-2/3} \frac{c_1}{(c_1 \beta)^{1/3}} y \left(\frac{x - \hat{x}_0(t)}{\lambda(t)} \right),$$

$$Q(x, t) = -h(x, t) \left[s_0(t_0 - t) + (t_0 - t)^{-1} \left(\frac{c_1}{h(x, t)} + \frac{2}{3}(x - \hat{x}_0) \right) \right], \quad (40)$$

where $\bar{x}_0(t) = 0.5s_0(t_0 - t)^2$, $\lambda(t) = 3(c_1\beta)^{1/3}(t_0 - t)^{2/3}$, $y \in I$.

The boundary condition $Q_\infty = -q_\infty(t_0 - t)^{-1}$ define c_1 : $c_1 = \frac{1}{3}q_\infty$. Comparing the first expression of (40) with (37), we find

$$y_{\max} = \frac{A\lambda_0}{q_\infty} < 1, \quad t_0 = \frac{1}{3} \sqrt{\frac{\lambda_0^3}{q_\infty \beta}}, \quad \zeta_{\max} = \frac{1}{2y_{\max}}, \quad x_0 = 0.5s_0t_0^2. \quad (41)$$

The time t_0 can be named ‘‘Time of the life of the wave’’, because for $t > t_0$ the wave does not exist. The physical meaning is clear. In the infinity we have the mass sources. The mass of the avalanche grow and moves contrary to the downslope direction. But we have on the basal surface the contrary flux that produces the wave which grows. The increase of the mass increases the capacity of the avalanche to move to the downslope direction. But the power of the mass flux grew too. The struggle of these factors causes the infinite increase of the amplitude of the wave. The law of the motion of the wave is obtained from (40)

$$x_{\max}(t) = 0.5s_0(t_0 - t)^2 + 3\zeta_{\max} \left(\frac{\beta q_\infty}{3} \right)^{1/3} (t_0 - t)^{2/3}.$$

The numerical results are obtained for following values of parameters: $s_0 = 0.2989$, $A = 0.083$, $\beta = 0.1$, $\lambda_0 = 1$, $q_\infty = 0.166$ and are illustrated by the Fig. 4. From (41) we found $y_{\max} = 0.5$, $t_0 = 2.587$, $x_0 = 1$.

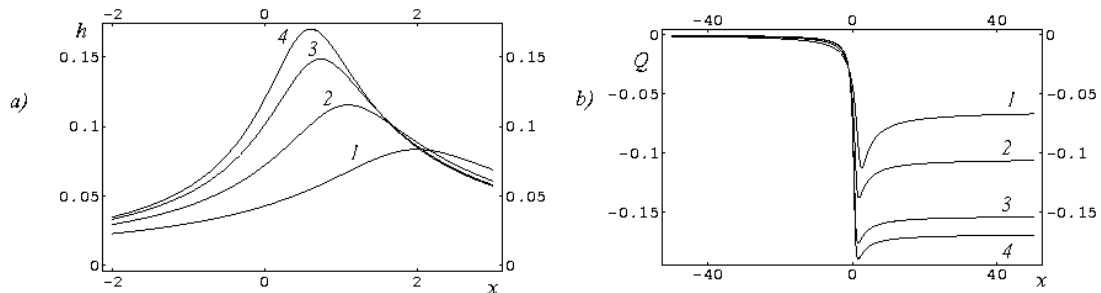


Figure 4. Behaviour of thickness a) and the mass flux b) during the ‘‘time of the life’’.

4.4 Example 4 ($\mu = 2$ in the general system (16), (17))

Let us consider the situation which is characterised by $\mu = 2$. This situation is interesting, because it allows us to model realistic case for the avalanches. For example, let us assume that

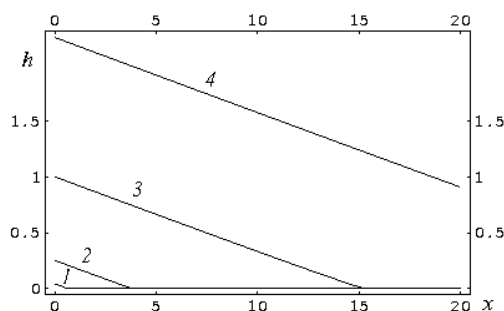


Figure 5. Dynamics of the thickness of the avalanche for $s_0 = 0.2989$, $h_0 = 0.01$ ($1 - t = 0$, $2 - t = 5$, $3 - t = 10$, $4 - t = 15$).

at the initial time the thickness of the avalanche is zero in the region $x > 0$ (there is a wall at point $x = 0$). The large mass of the granular material is in the region $x < 0$. When $t > 0$ the screen is lifted and suddenly removed, such that the thickness of the orifice is $h_0 t^2$. It is necessary to describe the evolution of free boundary of the avalanche for $x > 0$. For this purpose we take the solution (15) where $\mu = 2$

$$h = t^2 f(z), \quad \hat{Q} = t^3 q(z), \quad z = (x - 0.5s_0 t^2) t^{-2}. \quad (42)$$

The expression for z from (42) can be written in the form

$$z = xt^{-2} - 0.5s_0.$$

The latter relation shows that the region $z \leq -0.5s_0$ corresponds to the domain $x \leq 0$. Now, in order to resolve the problem we must find the solution of the system (16), (17) when $\mu = 2$ and with the boundary conditions

$$z = -0.5s_0, \quad f = h_0, \quad (43)$$

$$f = 0, \quad q = 0. \quad (44)$$

Fig. 5 illustrates the dynamics of the thickness of the avalanche for $s_0 = 0.2989$, $h_0 = 0.01$. Curve 1 corresponds to the moment $t = 3$; curve 2 is for $t = 5$; and curves 3, 4 are for $t = 10$, $t = 15$.

Acknowledgements

Publication of this work would not have been possible without financial assistance from Deutsche Forschungsgemeinschaft via its SFB program “Deformation and failure of metallic and granular media” and the Russian Fund of Fundamental Research (Grant N 00-01-00128).

- [1] Savage S.B. and Hutter K., The motion of a finite mass of granular material down a rough incline, *J. Fluid Mech.*, 1989, V.199, 177–215.
- [2] Savage S.B. and Hutter K., The dynamics of avalanches of granular materials from initiation to runout, *Acta Mech. Part I: Analysis*, 1991, V.86, 201–223.
- [3] Gray J.M.N.T., Wieland M. and Hutter K., Free surface flow of cohesionless granular avalanches over complex basal topography, *Proc. Roy. Soc. London A*, 1999, V.455, 1841–1874.
- [4] Gray J.M.N.T. and Tai Y.C., Particle size segregation, granular shocks and stratification patterns, *NATO ASI series, Physics of dry granular media*, Editors H.J. Herrmann et al., Kluwer Academic, 1998, 697–702.
- [5] Aksenov A.V., Baikov V.A., Chugunov V.A., Gazizov R.K. and Meshkov A.G., Lie group analysis of differential equations. Vol.2. Applications in engineering and physical sciences, Editor N.H. Ibragimov, CRC Press, 1995.
- [6] Hydon P.E., Symmetry methods for differential equations, Cambridge University Press, 2000.
- [7] Ibragimov N.H., Introduction to modern group analysis, Ufa, 2000.